# Observation of Droplet Size Oscillations in a Two-Phase Fluid under Shear Flow

Laurent Courbin and Pascal Panizza*
*Centre de Physique Optique Moléculaire Hertzienne, UMR 5798, 351 Cours de la Libération, 33400 Talence, France*

Jean-Baptiste Salmon
*Centre de Recherche Paul Pascal, Avenue Schweitzer, 33600 Pessac, France*
(Received 12 March 2003; published 9 January 2004)

Experimental observations of droplet size sustained oscillations are reported in a two-phase flow between a lamellar and a sponge phase. Under shear flow, this system presents two different steady states made of monodisperse multilamellar droplets, separated by a shear-thinning transition. At low and high shear rates, the droplet size results from a balance between surface tension and viscous stress, whereas for intermediate shear rates it becomes a periodic function of time. A possible mechanism for such kinds of oscillations is discussed.

DOI: 10.1103/PhysRevLett.92.018305 PACS numbers: 82.70.–y, 83.10.Gr, 83.60.Rs

Homogenizing immiscible fluids by the use of shear flow is an everyday experience and a fundamental step in the processing of soft materials [1]. By fragmenting large domains, the flow opposes the thermodynamics instability driving phase separation and leads to the formation of *nonequilibrium steady states* in which the coarsening is stopped [2]. Since the pioneering work of Taylor [3] on isolated Newtonian emulsions, the study of the rupture and deformation of isolated droplets under shear flow has drawn much attention. For Newtonian fluids, the dispersed phase forms generally somewhat deformed spherical droplets of the breakup size: $R \approx \chi/\eta\dot{\gamma}$, where $\chi$ is the surface tension between both phases, $\eta$ is the shear viscosity, and $\dot{\gamma}$ is the shear rate [3]. However, when the shear response of the fluids exhibits complexity as in semidilute entangled polymer solutions [4], near critical mixtures [5], lamellar-sponge phase-separated mixtures [6], or emulsions [7], other steady state structures such as cylindrical domains (known as the string phase), two-dimensional domains (ribbons phase), or colloidal crystals made of droplets are observed. Predicting the steady state domain morphology which results from the interplay between the flow, the surface tension, the volume fraction of the two phases, and their viscosities is a real challenge in nonequilibrium physics. Moreover, for a wide class of complex fluids, several different structures can be obtained under shear flow; these steady states are thus separated by out-of-equilibrium transitions. Depending on the nature of the rheological transition (shear thinning or shear thickening) and on the imposed dynamic variable (stress or shear rate), structural bistability and/or coexistence between structures characterized by shear banding can be seen [6,8,9]. Because energy is constantly brought into the system, these transitions are also expected to lead to richer behavior such as bifurcations to oscillatory states or even to chaos [10–14].

The purpose of this Letter is to show for the first time on two-phase flow that the droplet size can be a *periodic function of time*. Those oscillations are *asymptotic* (i.e., they do not correspond to a transient regime) and display a huge period of time, typically a few thousands of seconds.

We study a pseudobinary mixture made of sodium bis(2-ethylhexyl) sulfo-succinate (AOT) and brine (water and sodium chloride) [15]. At $T = 25\,^{\circ}\mathrm{C}$, for low salinities ($S \leq 14\ \mathrm{g\,l^{-1}}$), flat bilayers of AOT stack upon each other and a lamellar phase ($L_\alpha$) is observed. At high salinities ($S \geq 20\ \mathrm{g\,l^{-1}}$), the bilayers interconnect randomly and result in a Newtonian bicontinuous phase referred to in the literature as sponge phase (or $L_3$ phase) [16]. For intermediate salinities, coexistence between $L_\alpha$ and $L_3$ phases is found. We prepare solutions in the two-phase ($L_\alpha/L_3$) region with 20 wt. % AOT (from Fluka) and 80 wt. % brine ($S = 17\ \mathrm{g\,l^{-1}}$) and let them rest for a few weeks to reach equilibrium. Because of a density mismatch between the two phases, an interface appears and the volume fraction of $L_\alpha$ phase (65% at $T = 25\,^{\circ}\mathrm{C}$) can be measured directly from the observation of the position of this interface.

*Experiments.*—As previously described [17], small angle static light scattering experiments (SALS) are performed at imposed shear rate with a homemade transparent Couette cell, with gap $e = 1$ mm and inner radius $R_i = 16$ mm. In short, a circularly polarized laser beam (He-Ne, $\lambda = 632.8$ nm) passes through the cell along $\boldsymbol{\nabla v}$, the shear gradient direction, and probes the sample in only one of the gaps. The scattered pattern corresponding to light scattered in the velocity-vorticity $(\mathbf{v}, \mathbf{z})$ plane is digitalized, by means of a CCD videocamera for the frame acquisition. Experiments at imposed stress (rheology and SALS) are performed with a commercial rheometer (SR5, Rheometrics), using a transparent Mooney-Couette cell with gap $e = 0.7$ mm and inner radius $R_i = 14$ mm. To investigate the effect of flow on the ($L_\alpha/L_3$) phase region, the solution is stirred in order to obtain a macroscopic homogeneous mixture, before introducing it into the Couette cell and shearing it at a constant stress.

  

*Results.*—After a transient regime which is a few hours long, a steady state (i.e., $\dot{\gamma}$ does not any longer vary) is reached (see Fig. 1). This steady state I is characterized in SALS by a scattering ring with a well-defined sixfold modulation of its radial intensity (see Fig. 2). It does not depend on initial conditions and is determined only by the value of $\sigma$, the applied stress. If the flow is stopped, the ring persists during a few tens of minutes with same size, indicating that this shear-induced structure is metastable. Microscopic observations reveal that this homogeneous structure consists of monodisperse closed-compact multilamellar droplets [18] (inset of Fig. 2). The ring corresponds to the characteristic size of these closed-packed droplets, and its modulation shows the existence of a hexagonal order in the positions of the droplets. When the stress is increased, the value of the steady shear rate increases accordingly to $\dot{\gamma} \propto \sigma^2$ (indicating a shear thinning of the sample since the viscosity $\eta$ varies as $\eta = A_{\mathrm{I}}\dot{\gamma}^{-1/2}$, see Fig. 1). The size of the ring becomes larger and larger indicating that the steady droplet size $R$ decreases. At a well-defined stress $\sigma_c \approx 30$ Pa, a transition characterized by a jump in the measured shear rate occurs between steady state I and another steady state, labelled II. Above this transition, the scattering pattern consists also of a ring with six well-defined spots and the viscosity varies as $\eta = A_{\mathrm{II}}\dot{\gamma}^{-1/2}$. Although both steady states have similar rheological and microscopic features (see inset of Fig. 2), they can, however, be easily distinguished since the scattering ring and therefore the characteristic droplet size vary discontinuously at the transition (Fig. 2).

To study the nature of the transition between states I and II, we now perform the same experiment at fixed shear rate. Figure 2 shows the evolution of the steady droplet size $R$, deduced from SALS measurements, as a function of $\dot{\gamma}$. Two stationary branches, labelled I and II, are observed for $\dot{\gamma} \leq 100\ \mathrm{s}^{-1}$ and $\dot{\gamma} \geq 300\ \mathrm{s}^{-1}$, respectively. They correspond to the two steady states already observed in rheology (see Fig. 1). For intermediate shear rates (i.e., $100 \leq \dot{\gamma} \leq 300\ \mathrm{s}^{-1}$), very surprisingly, we do not observe any longer steady states, but instead *oscillatory states*. The size of the scattering ring oscillates indefinitely in time, indicating that the size of the droplets becomes a periodic function of time (Fig. 3).

Although these data have been recorded and digitalized for one day ($\approx 8 \times 10^4$ s), we have observed them visually over more than a week, with no amplitude and period shifts during this time. The droplet size increases very slowly (the typical duration of the growth is a few thousands of seconds long) and bursts out suddenly (in a few tens of seconds). During the continuous growth of the droplets, no spatial inhomogeneities, such as bands, are observed in the (**v**, **z**) planes. When the laser beam probing the structure is moved along the vertical **z** direction, the size of the scattering ring (and therefore the droplets size) remains constant in the whole cell. During the burst out of the droplets, the solution becomes turbid, the scattering ring vanishes, and horizontal bands are then observed in

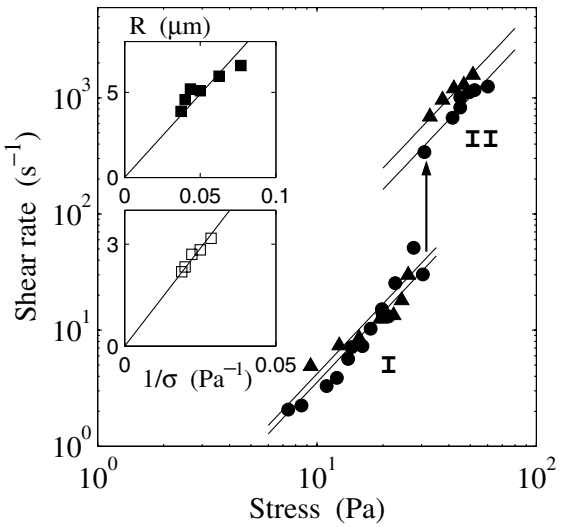


FIG. 1. Steady shear rate $\dot{\gamma}$ vs stress $\sigma$ for $T = 25\,^{\circ}\mathrm{C}$ and $S = 17\ \mathrm{g\,l^{-1}}$ (●) and $S = 17.15\ \mathrm{g\,l^{-1}}$ (▲), the equations of the solid lines are as follows (respectively for $S = 17\ \mathrm{g\,l^{-1}}$ and $S = 17.15\ \mathrm{g\,l^{-1}}$): $\dot{\gamma} = 0.042\sigma^2$ and $\dot{\gamma} = 0.036\sigma^2$ in region I, $\dot{\gamma} = 0.410\sigma^2$ and $\dot{\gamma} = 0.620\sigma^2$ in region II. For both steady states ($S = 17\ \mathrm{g\,l^{-1}}$ and $S = 17.15\ \mathrm{g\,l^{-1}}$), $\eta = A_i\dot{\gamma}^{-1/2}$ with $A_{\mathrm{I}} = 6.05\ \mathrm{Pa\,s^{1/2}}$ and $A_{\mathrm{I}} = 5.18\ \mathrm{Pa\,s^{1/2}}$, $A_{\mathrm{II}} = 1.73\ \mathrm{Pa\,s^{1/2}}$, and $A_{\mathrm{II}} = 1.33\ \mathrm{Pa\,s^{1/2}}$. Insets: Shown are the steady droplet sizes ($S = 17.15\ \mathrm{g\,l^{-1}}$) for region I (■) and II (□) versus $1/\sigma$. Solid lines are linear fits $R \propto 1/\sigma$.

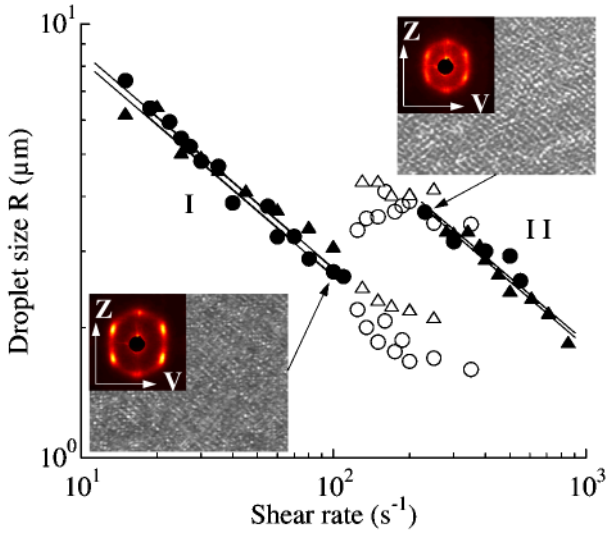


FIG. 2 (color online). Variation of $R$ the characteristic size measured from the position of the scattering ring in SALS with $\dot{\gamma}$. Circles and triangles correspond, respectively, to $S = 17\ \mathrm{g\,l^{-1}}$ and $S = 17.15\ \mathrm{g\,l^{-1}}$. Closed (▲,●) symbols represent steady states and open (△,○) symbols stand for the maxima and minima of the size during oscillations. The solid straight lines represent the best fits for $S = 17\ \mathrm{g\,l^{-1}}$ and $S = 17.15\ \mathrm{g\,l^{-1}}$, having slopes $-1/2$. Inset: Shown are the textures observed between crossed polarizers at $\dot{\gamma} = 100$ and $\dot{\gamma} = 230\ \mathrm{s^{-1}}$ and the corresponding SALS patterns.

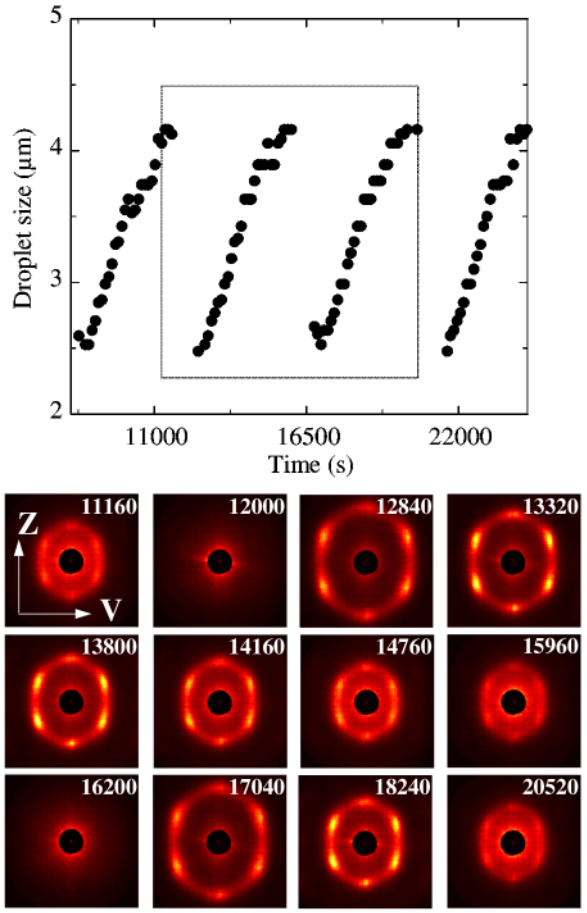


FIG. 3 (color online). Temporal evolution of $R(t)$, for $S = 17.15\ \mathrm{g\,l^{-1}}$ and $\dot{\gamma} = 130\ \mathrm{s^{-1}}$. Shown is the temporal evolution of the scattering pattern in the (**v**, **z**) plane.

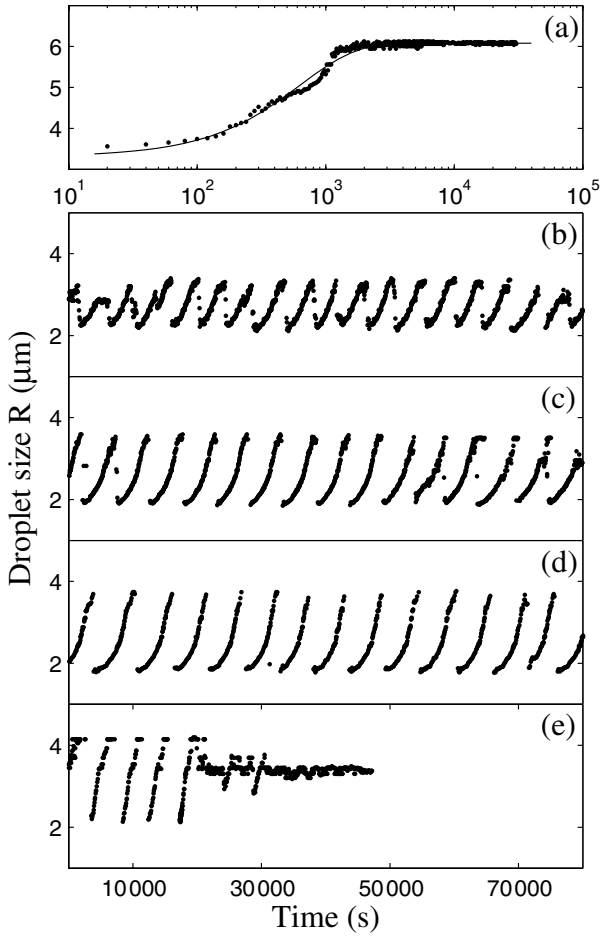


FIG. 4. Temporal evolution of $R(t)$, for (a) $\dot{\gamma} = 23\ \mathrm{s^{-1}}$ from an initial shear rate of $\dot{\gamma} = 54\ \mathrm{s^{-1}}$, the solid line corresponds to the best fit using an exponential expression: $R = 6.08 - 2.75\exp(-t/650)$, (b) $\dot{\gamma} = 125\ \mathrm{s^{-1}}$, (c) $\dot{\gamma} = 150\ \mathrm{s^{-1}}$, (d) $\dot{\gamma} = 175\ \mathrm{s^{-1}}$, and (e) to $\dot{\gamma} = 250\ \mathrm{s^{-1}}$ for $t < 20\,000$ s and $\dot{\gamma} = 280\ \mathrm{s^{-1}}$ for $t > 20\,000$ s.

the Couette cell. These reproducible oscillations are observed both upon increasing or decreasing the shear rate, for different parameters of the Couette cell (gaps and radii). The transition I-Oscillation occurs at a well-defined shear rate $\dot{\gamma}_c \approx 100\ \mathrm{s^{-1}}$, whereas the transition between Oscillation and II presents a hysteretic behavior for $230 \leq \dot{\gamma} \leq 300\ \mathrm{s^{-1}}$ (Fig. 2). Their period (a few thousands seconds) is many orders of magnitude larger than the period of rotation of the rotor (a few seconds) and varies with $\dot{\gamma}$ (see Fig. 4). These observations rule out any artifacts, such as a possible coupling with an external perturbation (building vibrations, temperature fluctuations, etc.). They clearly prove that the oscillations correspond to a nonlinear relaxation process.

*Discussion.*—These observations are very different from most unsteady flows reported in complex fluids, since they involve large relaxation oscillations between two different structural states (I and II) [19]: The droplet size oscillates. We believe that a better understanding of the transition I/II may provide us some insights to the oscillation mechanism. For both steady states, $R$ varies as $\dot{\gamma}^{-1/2}$, whereas $\eta \propto \dot{\gamma}^{-1/2}$. These two scaling laws suggest that the droplet size results in both states, from a balance between surface tension and viscous stress, yielding to the well-known relation [3]

$$R \approx \frac{\chi}{\eta\dot{\gamma}} = \frac{\chi}{\sigma}. \tag{1}$$

Within this picture, the surface tensions $\chi$ can be obtained from the slopes of the linear fits $R$ vs $1/\sigma$ displayed in the insets of Fig. 1. This estimation, respectively, leads to $\chi_{\mathrm{I}} \approx 9.5 \times 10^{-5}\ \mathrm{N\,m^{-1}}$ for state I and $\chi_{\mathrm{II}} \approx 11.5 \times 10^{-5}\ \mathrm{N\,m^{-1}}$ for state II. Both values are compatible with what is expected from a dimensional analysis, namely, $\chi \approx k_B T/l^2$, where $k_B T$ is the thermal energy and $l$ a correlation length of the mixture of the order of a few hundreds of angstroms (typically the smectic distance in the phase $L_\alpha$ or the pore size of the phase $L_3$). The transition I/II seems therefore related to a discontinuity in the surface tension between both coexisting phases. We believe that a compression of the multilamellar droplets occurs at this transition yielding to release of the solvent outside, and as a consequence to the change in $\chi$. Such a phenomenon which has already been evidenced in a $L_\alpha$ phase [20] is compatible with the

discontinuous jumps of the viscosity and the size observed at the transition I/II. It may also explain the turbidity enhancement occurring when the droplets burst. Within this picture, there is a critical pressure $\sigma_c$, above which the droplets compress and release water. More insights on such mechanism can be gained by considering, for instance, the following differential equation, describing a first-order phase transition induced by Laplace pressure between region I (uncompressed state, $\phi \approx 0$) and region II (compressed droplets, $\phi \approx 1$):

$$\dot{\phi} = -\frac{1}{\tau_1}\left(-\frac{\chi(\phi)/R - \sigma_c}{\sigma_c} - \alpha(2\phi - 1) + (2\phi - 1)^3\right). \quad (2)$$

Next to this transition, if the shear rate is increased, the size $R$ slightly decreases (since $R \propto \dot{\gamma}^{-1/2}$). Then, the Laplace pressure $\chi/R$ becomes higher than $\sigma_c$ and water is expelled from the droplets. This water release decreases the viscosity and consequently the viscous stress. Because of Eq. (1), the droplet size then increases again and the Laplace pressure decreases. As a result, the water goes back into the droplets and the same mechanism starts over, leading to sustained oscillations. Because permeation of water through membranes is a very slow process [21], such a scenario may explain the very large time scales involved in our observations, as suggested in Ref. [10].

In a first approach, for simplicity's sake, we consider that the temporal evolution of $R(t)$ is driven by the following first-order kinetics:

$$\dot{R} = -\frac{1}{\tau_2}\left(R - \frac{\chi(\phi)}{\eta(\phi, \dot{\gamma})\dot{\gamma}}\right), \quad (3)$$

with $\chi(\phi) = \chi_{\mathrm{I}}(1 - \phi) + \chi_{II}\phi$, and $\eta(\phi, \dot{\gamma}) = A(\phi)\dot{\gamma}^{-1/2}$, where $A(\phi) = A_{\mathrm{I}}(1 - \phi) + A_{\mathrm{II}}\phi$. Taking for $A_{\mathrm{I}}, A_{\mathrm{II}}, \chi_{\mathrm{I}}, \chi_{\mathrm{II}}, \sigma_c$ the values found experimentally (Figs. 1 and 2) and $\tau_2 = 650$ s (Fig. 4), our simplified two equations reproduce the two steady branches observed experimentally for both the droplet size and the viscosity. For intermediate shear rates, in a given range of the $\alpha$ and $\tau_1$ parameters, it may also lead to sustained droplet size oscillations [22]. The transient banding behavior observed during the fast burst of the droplets suggests that an overall description requires the setup of space and time-dependent nonlinear coupled differential equations. Such approaches are currently being developed with success by theorists to describe spatiotemporal flows of complex fluids [12,13]. We hope that our experiments on a model system will stimulate such theoretical researches.

In conclusion, we have shown, in a two-phase flow, the existence of *nonlinear structural oscillatory states* for which droplet size is a periodic function of time. These oscillations are monitored by a shear-induced change of the surface tension between both phases. We therefore believe that such a mechanism is general and may also be found in other systems exhibiting shear-induced phase transitions such as, for instance, micellar solutions, liquid crystals, liquid crystal polymers, etc.

As a final comment, this new result raises now an important question: Can the droplet size display *chaotic* behavior? We believe that this question will be a major topic of research in the study of *rheochaos* [12] in the near future.

We thank T. Douar and M. Winckert for technical assistance. We acknowledge fruitful discussions with A. Benayad, A. Colin, J.-P. Delville, and J. Rouch.

*Electronic address: p.panizza@cpmoh.u-bordeaux1.fr

[1] R. G. Larson, *The Structure and Rheology of Complex Fluids* (Oxford University Press, New York, 1999).
[2] A. Onuki, J. Phys. Condens. Matter **9**, 6119 (1997).
[3] G. I. Taylor, Proc. R. Soc. London A **146**, 501 (1934).
[4] T. Hashimoto, K. Matsuzaka, and E. Moses, Phys. Rev. Lett. **74**, 126 (1995).
[5] K. Y. Min, J. Stavans, R. Piazza, and W. I. Goldburg, Phys. Rev. Lett. **63**, 1070 (1989).
[6] G. Cristobal, J. Rouch, A. Colin, P. Panizza, and T. Narayanan, Phys. Rev. E **62**, 3871 (2000); Phys. Rev. E **64**, 011505 (2001).
[7] T. G. Mason and J. Bibette, Phys. Rev. Lett. **77**, 3481 (1996).
[8] D. Bonn, J. Meunier, O. Greffier, A. Al-Kahwaji, and H. Kellay, Phys. Rev. E **58**, 2115 (1998), and references therein.
[9] P. D. Olmsted and C.-Y. D. Lu, Phys. Rev. E **56**, 55 (1997); P. D. Olmsted, Europhys. Lett. **48**, 339 (1999), and references therein.
[10] A.-S. Wunenburger, A. Colin, J. Leng, A. Arnéodo, and D. Roux, Phys. Rev. Lett. **86**, 1374 (2001); J.-B. Salmon, A. Colin, and D. Roux, Phys. Rev. E **66**, 031505 (2002).
[11] R. Bandyopadhyay, G. Basappa, and A. K. Sood, Phys. Rev. Lett. **84**, 2022 (2000).
[12] D. A. Head, A. Ajdari, and M. E. Cates, Phys. Rev. E **64**, 061509 (2001); Europhys. Lett. **57**, 120 (2001).
[13] G. Picard, A. Ajdari, L. Bocquet, and F. Lequeux, Phys. Rev. E **66**, 051501 (2002).
[14] M. Grosso, R. Keunings, S. Crescitelli, and P. L. Maffettone, Phys. Rev. Lett. **86**, 3184 (2001).
[15] O. Gosh and C. A. Miller, J. Phys. Chem. **91**, 4528 (1987).
[16] G. Porte, J. Phys. Condens. Matter **4**, 8649 (1992).
[17] L. Courbin, J.-P. Delville, J. Rouch, and P. Panizza, Phys. Rev. Lett. **89**, 148305 (2002).
[18] L. Courbin, R. Pons, J. Rouch, and P. Panizza, Europhys. Lett. **61**, 275 (2003).
[19] Structural oscillations between a disordered and an ordered state have been reported by Wunenburger *et al.* in a $L_\alpha$ phase at fixed stress [10].
[20] O. Diat, D. Roux, and F. Nallet, Phys. Rev. E **51**, 3296 (1995); P. Sierro and D. Roux, Phys. Rev. Lett. **78**, 1496 (1997).
[21] J. Leng, F. Nallet, and D. Roux, Eur. Phys. J. E **4**, 77 (2001).
[22] L. Courbin, P. Panizza, and J.-B. Salmon (to be published).